



Superplastic forming of titanium alloys at 700°C

M. R. Shagiev[†], A. A. Kruglov, O. A. Rudenko, M. A. Murzinova

[†]marat@imsp.ru

Institute for Metals Superplasticity Problems of the RAS, Ufa, 450001, Russia

The formability of the novel Ti-1.5Al-1.5V-2.75Fe-3.0Mo-0.25Ni-0.1B alloy and the commercial Ti-6Al-4V alloy at 700°C was evaluated in the present study. Experiments have demonstrated the possibility of superplastic forming of both alloys with a fine-grained microstructure at 700°C and a constant argon gas pressure $p=2$ MPa. However, the forming time for the novel alloy was only a few minutes ($\tau=235$ s), while for the Ti-6Al-4V it amounted almost 2.5 hours ($\tau=8700$ s). The better formability of the novel alloy at 700°C compared to the commercial one is in good agreement with the results of computer simulations performed earlier and is mainly due to an increased content of the β phase. Microstructural analysis showed that low-temperature superplastic forming was accompanied by the development of spheroidization and recrystallization processes. It is important that recrystallization did not lead to a significant grain growth and provided an increase in the structure homogeneity and randomization of the rolling texture. The most significant improvement of microstructure homogeneity after forming at 700°C was observed in the Ti-6Al-4V alloy with the initial partially recrystallized structure.

Keywords: superplastic forming, titanium alloys, forming time, microstructure, texture.

1. Introduction

Superplastic forming (SPF) is a promising technology for the production of complex-shaped parts from hard-to-deform alloys. However, its wide application for commercial ($\alpha+\beta$)-titanium alloys is limited by the need to carry out the process at high temperatures (850–950°C) and low strain rates (10^{-3} – 10^{-4} s⁻¹) [1–3]. A decrease in the SPF temperature down to 650–750°C can be achieved by the formation of an ultrafine-grained structure in materials [4,5], but this is very expensive and laborious. As it was shown recently [6], due to the use of protective atmospheres, which slow down the surface oxidation of preforms, commercial Ti-6Al-4V sheets with a fine-grained structure can also be formed at a temperature as low as 700°C, but this significantly increases the forming time that is not technological. Meanwhile, a new approach to design titanium alloys with improved superplastic properties through optimization of their chemical and phase compositions was proposed in [7]. Based on it, compositions of novel alloys were determined, trial sheets with a homogeneous fine-grained structure were produced, and their mechanical properties were studied. It was shown that those alloys had improved superplastic properties at temperatures of 650–750°C and strain rates of $\sim 10^{-3}$ – 10^{-2} s⁻¹. According to the results of computer simulations, novel alloys have a good formability at temperatures of 700 and 750°C, which is much better than that of the commercial Ti-6Al-4V alloy with a fine-grained structure [7]. The aim of the present work was to evaluate experimentally

the formability of titanium alloys at 700°C and to study their microstructure and microtexture before and after SPF.

2. Materials and experimental methods

The starting materials were a commercial sheet of the VT6c (hereinafter referred to as Ti-6Al-4V) alloy manufactured by the VSMPO-AVISMA corporation and a sheet of the novel titanium alloy designated in [7] as Alloy 2 and produced according to technological regimes described in [4]. The thickness of both sheets was 1 mm. The chemical compositions of the studied alloys are given in Table 1.

The results of preliminary studies showed that both alloys had a fine-grained structure with sizes of α - and β -phase particles less than 5 μ m. However, the volume fraction of β phase differed significantly and amounted to $V_\beta=37\%$ in the novel alloy and $V_\beta=7\%$ in the commercial one. Both alloys exhibited the signs of superplasticity during tensile tests at 700°C and initial strain rates of 4.2×10^{-4} – 8.3×10^{-3} s⁻¹. Under these conditions, the novel alloy had the total elongations $\delta=632$ – 1307% and the steady-state flow stresses $\sigma_s=35$ – 90 MPa [7], while the Ti-6Al-4V alloy possessed $\delta=105$ – 296% and $\sigma_s=120$ – 280 MPa [8].

The experimental SPF of model hemispheres with a radius of 35 mm was carried out in a vacuum furnace at $T=700^\circ\text{C}$ and a constant argon pressure $p=2$ MPa according to the scheme given in [9,10]. Formability was assessed by the forming time of hemispheres.

Table 1. Chemical composition of the alloys.

Alloy	Content of alloying elements, wt.%								
	Ti	Al	V	Fe	Ni	Mo	Si	B	O
Novel alloy	base	1.5	1.5	2.75	0.25	3.0	0	0.1	<0.2
Ti-6Al-4V	base	6.3	3.7	<0.25	-	-	<0.15	-	<0.15

Microstructural analysis of the sections of sheets and hemispheres was performed using a TESCAN MIRA 3 LMH FEG scanning electron microscope equipped with backscattered electron (BSE) and electron backscatter diffraction (EBSD) detectors. EBSD scanning was performed with a step of 0.1 μm to obtain crystal orientation maps and with a step of 0.5 μm for microtexture studies. The equivalent diameter was taken as the grain size. Quantitative analysis of the microstructure was performed in accordance with the recommendations in [11,12].

3. Results and discussion

The experiments showed the possibility of forming at 700°C of both the Ti-1.5Al-1.5V-2.75Fe-3.0Mo-0.25Ni-0.1B alloy with improved superplastic properties and the Ti-6Al-4V alloy (Fig. 1). However, the time of forming a hemisphere out of the novel alloy was only $\tau = 235$ s, while for the Ti-6Al-4V it was 37 times longer, $\tau = 8700$ s, that is in good agreement with the results of computer simulations [7]. For both alloys, with the initial thickness of preform $S_0 = 1$ mm, the thickness of the hemisphere at the edge of the fixing zone (the area with the lowest strain) was $S_{\max} = 0.78 - 0.79$ mm, and the thickness at the pole of the hemisphere (the area with the largest strain) was $S_{\min} = 0.27 - 0.29$ mm, which is quite typical for the SPF of hemispheres with a constant pressure and rigid clamping of the flange of the sheet preform [13]. For industrial SPF processes, special techniques are used to minimize the variation in thickness [14], but this task is out of the scope of the present work.

The decrease in thickness of the preforms was used to estimate the strain rate during SPF. For the novel alloy it was about 10^{-3} s^{-1} indicating that SPF was performed under optimal superplastic conditions [7]. For the fine-grained Ti-6Al-4V alloy, the forming temperature $T = 700^\circ\text{C}$ corresponded to the lower temperature limit of superplasticity [1, 3]. Therefore, its SPF was carried out at much lower strain rates $10^{-5} - 10^{-4} \text{ s}^{-1}$, close to creep rates.

The better formability of the novel alloy compared to that of the commercial Ti-6Al-4V can be easily explained by the higher volume fraction of the soft β phase, which at 700°C reaches $V_\beta = 37 - 41\%$ in the Ti-1.5Al-1.5V-2.75Fe-3.0Mo-0.25Ni-0.1B

alloy [7], while in the Ti-6Al-4V alloy only $V_\beta = 15 - 20\%$ [15,16].

Structural analysis revealed that the alloys differed not only by their phase compositions. Typical BSE images, crystal orientation maps of the microstructure and microtexture of alloys before SPF are shown in Figs. 2 and 3, while that for conditions after SPF are given in Figs. 4 and 5. One can see that in the sheets of both alloys, the particles of α and β phases were elongated in the rolling direction (Figs. 2a and 3a). However, a recrystallized structure was formed in the novel alloy (Fig. 2b), whereas the structure of the commercial alloy was partially recrystallized: along with fine equiaxed grains, it contained large elongated α grains with a developed subgrain structure (Fig. 3b). The average grain sizes in the sheets of both alloys were close and amounted to $d_{\text{av}} = 0.9 \mu\text{m}$ for the novel alloy and $d_{\text{av}} = 1.4 \mu\text{m}$ for the Ti-6Al-4V. At the same time, the grain size distributions were significantly different (Fig. 6). In the Ti-1.5Al-1.5V-2.75Fe-3.0Mo-0.25Ni-0.1B sheet, it was lognormal, and the main analyzed area was occupied by grains with sizes from 1 to 5 μm . The distribution of grain sizes in the Ti-6Al-4V sheet was bimodal: grains with sizes from 1 to 7 μm and from 7 to 25 μm occupied almost the same area.

The microtexture in the sheets (Figs. 2c and 3c) was typical for titanium alloys and depended on the rolling scheme, volume fractions and chemical composition of α and β phases [16–20]. In the cross-rolled Ti-1.5Al-1.5V-2.75Fe-3.0Mo-0.25Ni-0.1B sheet, a predominantly basal texture was formed in the α phase (Fig. 2c) providing the isotropy of mechanical properties in the sheet plane, which is very important for SPF. Rolling of the Ti-6Al-4V sheet was apparently performed in one direction, and, in addition to the basal texture, a transverse component of the texture was also observed in the α phase (Fig. 3c).

During SPF and subsequent slow cooling of the hemispheres in a vacuum furnace, the processes of spheroidization, recovery and recrystallization developed in both alloys that was accompanied by the microtexture randomization (see pole figures in Figs. 2–5). This is more typical for processing at higher temperatures [20]. As a result of spheroidization of the α - and β -phase particles, metallographic texture of the sheets weakened (see BSE images in Figs. 2–5). Due to the occurrence of recovery processes, a significant reduction in the extent of low-angle

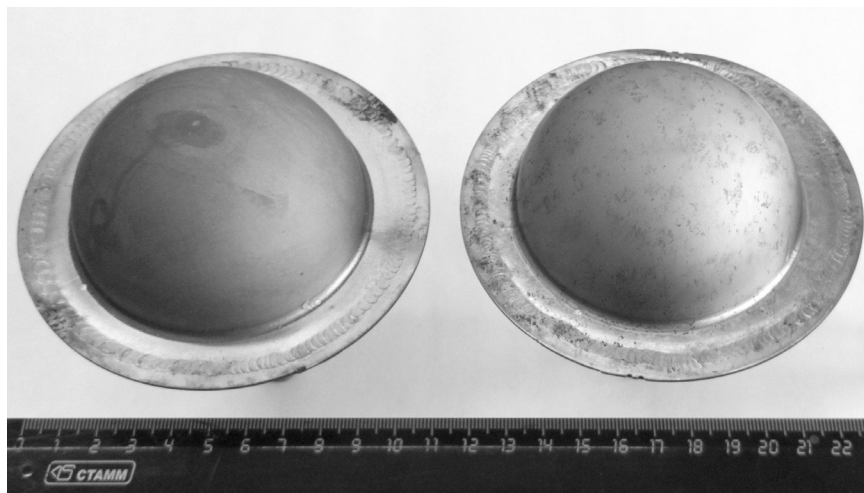


Fig. 1. Hemispheres produced by SPF at $T = 700^\circ\text{C}$ and $p = 2$ MPa from the Ti-6Al-4V sheet (left) and the Ti-1.5Al-1.5V-2.75Fe-3.0Mo-0.25Ni-0.1B sheet (right).

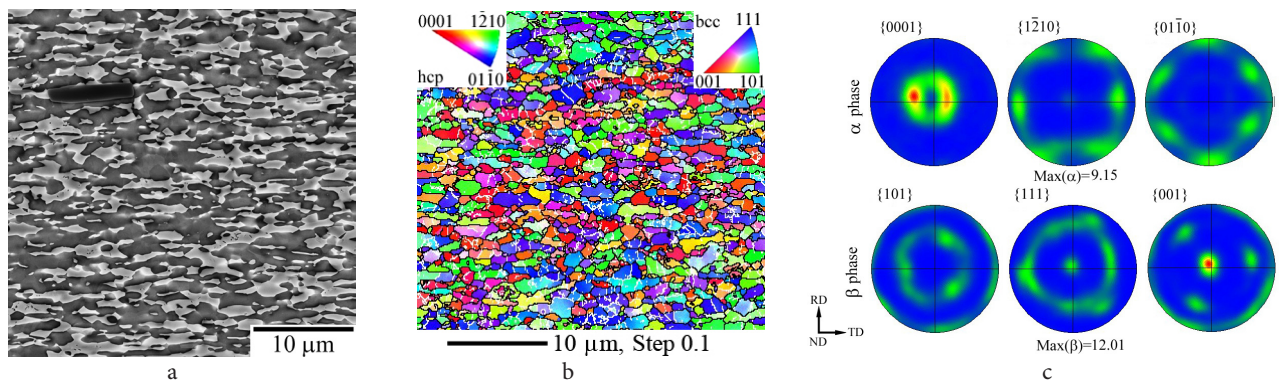


Fig. 2. (Color online) BSE image (a), crystal orientation map of the microstructure in the longitudinal section (b), and pole figures from the plane of the Ti-1.5Al-1.5V-2.75Fe-3.0Mo-0.25Ni-0.1B sheet (c). The color codes for α and β phases are shown in the upper corners of (b) and are the same for all orientation maps below.

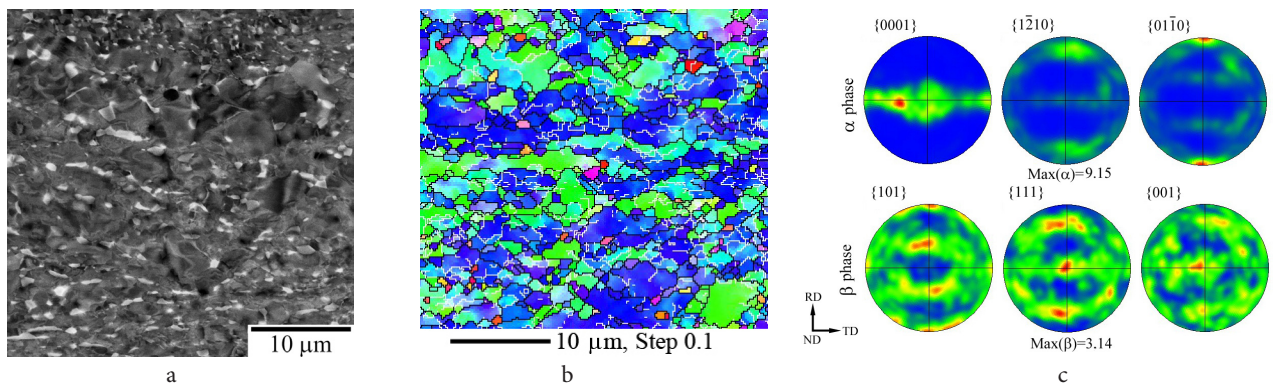


Fig. 3. (Color online) BSE image (a), crystal orientation map of the microstructure in the longitudinal section (b), and pole figures from the plane of the Ti-6Al-4V sheet (c).

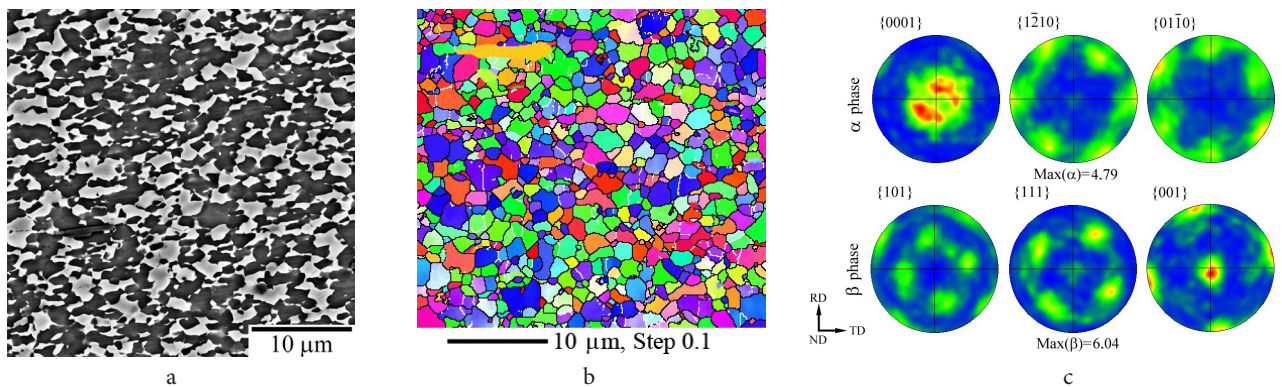


Fig. 4. (Color online) BSE image (a), crystal orientation map of the microstructure in the pole section (b), and pole figures from the surface of hemisphere out of the Ti-1.5Al-1.5V-2.75Fe-3.0Mo-0.25Ni-0.1B alloy (c).

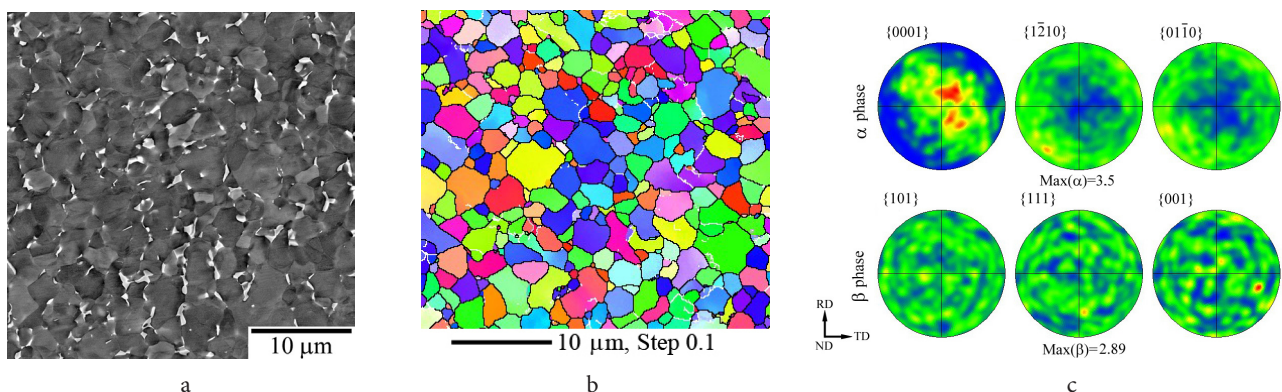


Fig. 5. (Color online) BSE image (a), crystal orientation map of the microstructure in the pole section (b), and pole figures from the surface of hemisphere out of the Ti-6Al-4V alloy (c).

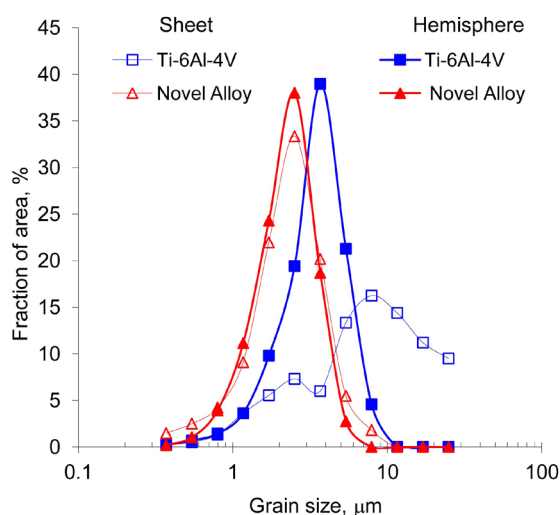


Fig. 6. (Color online) Grain size distribution in Ti-1.5Al-1.5V-2.75Fe-3.0Mo-0.25Ni-0.1B and Ti-6Al-4V alloys before and after SPF at $T=700^{\circ}\text{C}$.

boundaries was observed (see orientation maps in Figs. 2–5). Recrystallization did not lead to a substantial grain growth in both alloys and had the greatest effect on the microstructure of the Ti-6Al-4V alloy (Figs. 4b, 5b, and 6). After SPF, a homogeneous microstructure with a lognormal distribution of grain sizes was formed in it, and the main analyzed area was occupied by grains with sizes from 1.5 to 7 μm (Fig. 6). It can be expected that the homogeneous fine-grained microstructure formed after SPF will have higher performance properties compared to those of the commercial Ti-6Al-4V sheet [16, 20]. The distribution of grain sizes in the novel alloy after SPF did not change fundamentally, it only became slightly narrower (Fig. 6). It should be noted that the deformation during SPF had the main influence on the development of spheroidization and recrystallization [21], since the recovery processes prevailed in the fixing zone of the hemispheres, which were heat treated at 700°C without straining.

4. Conclusions

The possibility of superplastic forming of the novel Ti-1.5Al-1.5V-2.75Fe-3.0Mo-0.25Ni-0.1B alloy and the commercial Ti-6Al-4V alloy at a relatively low temperature $T=700^{\circ}\text{C}$ has been demonstrated. It was shown that the novel alloy with improved superplastic characteristics had a better formability compared to the Ti-6Al-4V: the forming time of a model hemisphere with radius of 35 mm at $T=700^{\circ}\text{C}$ and $p=2\text{ MPa}$ for the first alloy was only several minutes ($\tau=235\text{ s}$), and for the second — almost 2.5 hours ($\tau=8700\text{ s}$). This is in good agreement with the results of computer simulations performed earlier and is mainly due to the higher volume fraction of the β phase in the novel alloy.

Microstructural analysis revealed that superplastic forming of the studied alloys at 700°C did not lead to coarsening of the structure, while its homogeneity was increased and randomization of the rolling texture was observed. The most significant increase in the homogeneity of microstructure after forming was observed in the commercial Ti-6Al-4V sheet with the initial partially recrystallized structure.

Acknowledgements. The work was performed using the facilities of shared services center “Structural and Physical-Mechanical Studies of Materials” within the State Assignment of the Institute for Metals Superplasticity Problems of the Russian Academy of Sciences.

References

1. O.A. Kaibyshev. Superplasticity of Alloys. Intermetallides and Ceramics. Berlin, Springer-Verlag (1992) 317 p. [Crossref](#)
2. A. Barnes. Journal of Materials Engineering and Performance. 16, 440 (2007). [Crossref](#)
3. E. Alabort, D. Putman, R.C. Reed. Acta Materialia. 95, 428 (2015). [Crossref](#)
4. G.A. Salishchev, R.M. Galeev, O.R. Valiakhmetov, R.V. Safiullin, R.Ya. Lutfullin, O.N. Senkov, F.H. Froes, O.A. Kaibyshev. Journal of Materials Processing Technology. 116, 265 (2001). [Crossref](#)
5. P.N. Comley. Materials Science Forum. 447–448, 233 (2004). [Crossref](#)
6. M.R. Shagiev, M.A. Murzinova. Letters on Materials. 11 (4s), 553 (2021). [Crossref](#)
7. E. Alabort, D. Barba, M.R. Shagiev, M.A. Murzinova, R.M. Galeev, O.R. Valiakhmetov, A.F. Aletdinov, R.C. Reed. Acta Materialia. 178, 275 (2019). [Crossref](#)
8. M.R. Shagiev, A.A. Kruglov, E. Alabort, F.U. Enikeev, R.M. Shagiev. In: Ultrafine-grained and Nanostructured Materials (Ed. by A.A. Nazarov). Ufa, Bashkir State University (2020) p. 193. (in Russian)
9. F.U. Enikeev, A.A. Kruglov. International Journal of Mechanical Sciences. 37 (5), 473 (1995). [Crossref](#)
10. O.A. Rudenko, A.A. Kruglov, R.V. Safiullin, O.R. Valiakhmetov, R.Ya. Lutfullin. Forging and Stamping Production. Material Working by Pressure. 4, 5 (2006). (in Russian)
11. S.A. Saltykov. Stereometric metallography. Moscow, Metallurgy (1970) 376 p. (in Russian)
12. M.A. Shtremel. Strength of Alloys. Part 1: Defects of the Lattice. Moscow, MISIS (1999) 384 p. (in Russian)
13. Superplastic Forming of Structural Alloys (Ed. by N.E. Paton, C.H. Hamilton). Warrendale, PA, The Metallurgical Society of AIME (1982) 414 p.
14. G.R. Murzina, V.R. Ganieva, A.A. Kruglov, F.U. Enikeev. Letters on Materials. 11 (4s), 548 (2021). [Crossref](#)
15. N. Saunders. In: Titanium'95: Science and Technology (Ed. by P. Bleckinsop, W.J. Evans, H.M. Flower). London, Institute of Materials (1996) 2167 p.
16. G. Lütjering, J.C. Williams. Titanium, 2nd ed. Berlin, Springer-Verlag (2007) 449 p.
17. U. Zwicker. Titanium and its alloys. Moscow, Metallurgy (1979) 512 p. (in Russian)
18. Q. Chao, P.D. Hodgson, H. Beladi. Materials Science and Engineering A. 694, 13 (2017). [Crossref](#)
19. J. Zhao, K. Wang, K. Huang, G. Liu. Materials Characterization. 151, 429 (2019). [Crossref](#)
20. S.L. Semiatin. Metallurgical and Materials Transactions A. 51, 2593 (2020). [Crossref](#)
21. S.V. Zharebtsov, E.A. Kudryavtsev, G.A. Salishchev, B.B. Straumal, S.L. Semiatin. Acta Materialia. 121, 152 (2016). [Crossref](#)